Equilibria of 3-Pyridylmethanol with Copper(II). A Comparative Electron Spin Resonance Study by the Decomposition of Spectra in Liquid and Frozen Solutions

Rastislav Šípoš,[†] Terézia Szabó-Plánka,*[,‡] Antal Rockenbauer,[§] Nóra Veronika Nagy,[§] Jozef Šima,[†] Milan Melník,[†] and István Nagypál[‡]

Department of Inorganic Chemistry, Slovak Technical University, Bratislava, Slovakia, Department of Physical Chemistry, University of Szeged, Rerrich Béla tér 1, H-6720 Szeged, Hungary, and Chemical Research Center, Institute of Structural Chemistry, Hungarian Academy of Sciences, Budapest, Hungary

Received: June 13, 2008; Revised Manuscript Received: July 29, 2008

The copper(II)−3-pyridylmethanol (L) system was investigated in aqueous solution by two-dimensional ESR evaluation at 298 K, and computer simulation of the individual anisotropic spectra at 77 K. The data revealed that the paramagnetic copper(II) complexes $[CuL]^{2+}$, $[CuL_2]^{2+}$, $[CuL_3]^{2+}$, and $[CuL_4]^{2+}$ are formed up to pH ≈ 7 at a moderate or high excess of ligand. As compared with chelating ligands, two differences were observed for the complexation of 3-pyridylmethanol with copper(II): (1) In contrast with the well-resolved spectra in frozen solution, considerable line-broadening and distortion of the spectral shapes were seen at 298 K, which was interpreted in terms of isomeric equilibria and the medium-rate interconversion of various complexes on the ESR time-scale. (2) At low temperature, there were dramatic changes in the concentration distribution, the minor complexes with higher numbers of coordinating ligands ($[CuL_3]^{2+}$ and in particular $[CuL_4]^{2+}$) becoming strongly favored. This phenomenon is explained by the significant differences in the formation enthalpy values of various species, shifting the equilibria according to the van't Hoff equation, and a significant undercooling in the course of fast freezing of the solution, which enhances the changes of the concentration distribution.

1. Introduction

After it was recognized that copper(II), an anti-inflammatory agent itself, enhances the pharmaceutic effect of most organic nonsteroidal anti-inflammatory drugs (NSAIDs), a number of copper(II)-based NSAID molecules were developed.[1] One of the NSAIDs in current use is 3-pyridylmethanol (also known as β-pyridylcarbinol, nicotinyl alcohol or ronicol).[2] Clinical studies of 3-pyridylmethanol date back to 1952, when its application for the conservative therapy of ocular burns was described.[3] It is also suitable for the treatment of hypercholesterolemia, hyperlipidemia, hypertriglyceridemia and cardiovascular diseases.[4,5] There is good evidence that the vasodilator and fibrinolytic actions of 3-pyridylmethanol in humans and animals are mediated by the release of endogenous prostacyclin.[6] Cu(II) complexes that act as scavengers of reactive oxygen species are expected to replace the more toxic gold compounds in the treatment of arthritis. A mixed-ligand Cu(II) complex of 3-pyridylmethanol and niflumic acid has been demonstrated to be an effective drug in rats with adjuvant arthritis.[7] In the solid state, the main binding site of 3-pyridylmethanol in its complexes is the pyridyl N. In some cases, 3-pyridylmethanol forms bridges between the Cu(II) ions in the crystal lattice, when its alcoholic group is also coordinated; proton loss from this group has not been observed.[8−13] The pharmaceutical importance of 3-pyridylmethanol has stimulated studies of its complexation in solution, where the conditions are closer to those in biological systems, compared with the investigations of crystalline samples.

For studies of paramagnetic complex equilibria in solution, a special spectrum-deconvolution technique, two-dimensional (2D) ESR simulation,[14] has been elaborated. Its name stems from the fact that the intensity is treated as a function of two variables, the field and the concentration: all ESR spectra recorded at various metal, ligand and H^+ concentrations are simulated in the same optimization procedure, the magnetic parameters and formation constants of each ESR-active species being fitted simultaneously. The method has been applied to a number of systems:[14−21] new major and minor species have been identified and characterized, including coordination and geometric isomers of various complexes. For the equilibria of chelating ligands, the slow-exchange criterion is fulfilled: the interconversion of various species is slow on the ESR time scale, and therefore the measured spectra can be described well as the sums of the spectra of the individual species, weighted by their concentrations in the solution. This experience is in good accordance with the results of NMR relaxation studies:[22−24] from the dissociation rate constants obtained, a typical lifetime of $\geq 10^{-8}$ s can be estimated for a number of Cu(II) complexes with mono- and bidentate ligands. In contrast with the ligands studied by the 2D simulation method to date, 3-pyridylmethanol cannot form chelate rings with the metal ion.

The aims of our studies were to obtain information via the 2D ESR evaluation method on the complex equilibria of 3-pyridylmethanol with Cu(II), including the stability and coordination modes of various species, and to compare the general features of the ESR spectra for the complexes of this nonchelating ligand with those of chelate complexes of Cu(II) studied earlier. Computer simulation of anisotropic ESR spectra recorded in frozen solution at 77 K was carried out to elucidate the effects of temperature on these equilibria.

* Corresponding author. Tel: +36-62-546368. Fax: +36-62-544652. E-mail address: szabot@chem.u-szeged.hu.
[†] Slovak Technical University.
[‡] University of Szeged.
[§] Hungarian Academy of Sciences.

10.1021/jp805210v CCC: $40.75
Published on Web 09/10/2008

2. Experimental Section

2.1. Materials. 3-Pyridylmethanol of analytical grade was purchased from Aldrich. It is symbolized by L in its neutral form when the compositions of its various complexes are formulated below. Doubly deionized water was used as solvent. Other reagents of analytical grade were supplied by Aldrich or Sigma and used as received.

2.2. ESR Titrations. The titrations were carried out in a circulating system to ensure that all spectra were recorded under identical conditions, and so the signal intensity be proportional to the complex concentration in the whole series of spectra. The measurements were carried out in an air-conditioned room at 298 ± 0.2 K in the pH range 2 to 5.5−7; each titration was finished when the opalescence of the solution indicated that Cu(II) hydroxide had started to precipitate. The total (analytical) Cu(II) concentration T_{Cu} was 0.005 M, and the total ligand concentration T_L was 0.010, 0.025 or 0.100 M. KCl (0.2 M) was applied as background electrolyte. The pH was decreased first down to about 2 by adding HCl (0.2 M) to suppress the formation of metal complexes. Then NaOH (0.2 M) portions were added by a Metrohm Dosimat 765 automatic buret. The pH was measured to an accuracy of 0.01 pH unit, using a Radiometer PHN 240 pH meter equipped with a Metrohm LL combined microelectrode, which was calibrated with IUPAC Standard Buffers (Radiometer). The solutions were kept under an argon atmosphere; the bubbles of the gas mixed their components. A Masterflex CL peristaltic pump ensured the circulation of the solution through the capillary tube in the cavity. The ESR spectra were recorded after 2 min of circulation at the chosen pH values, using an X-band Bruker EleXsys E500 instrument. The complex formation is characterized by the set of the formation constants $\beta_{Cu_pL_qH_r}$, the equilibrium constants for the following general equilibrium process:

$$pCu + qL + rH \rightleftharpoons Cu_pL_qH_r$$

$$\beta_{Cu_pL_qH_r} = \frac{[Cu_pL_qH_r]}{[Cu]^p[L]^q[H]^r}$$

where Cu denotes the metal ion and L the nonprotonated ligand molecule. (Charges are omitted for simplicity.)

2.3. ESR Measurements at 77 K. Samples of 0.15 cm^3, taken at various pH from the mixtures titrated at 298 K, were placed in liquid nitrogen after 0.05 cm^3 methanol had been added to promote glass formation during freezing. The congelation of the solution took place within 5 s. The ESR spectra were then recorded at 77 K with the same spectrometer as above.

2.4. Evaluation of ESR Spectra in Fluid Solution. The analysis of the spectra was preceded by a correction for the curve of the capillary tube in the cavity, filled with distilled water, and by a numerical field shift to obtain the spectra at a common frequency. The series of ESR spectra were then evaluated by using the 2DEPR program.[14] The ESR spectra of the various species were described by the parameters g_0, the Cu hyperfine coupling constant A_0, the N superhyperfine coupling constant a_{N0}, and the relaxation parameters α, β and γ relating to the linewidths of the Cu hyperfine multiplet as $W_{M_I} = \alpha + \beta M_I + \gamma M_I^2$ (M_I is the magnetic quantum number of the Cu nucleus). As we used a natural mixture of Cu isotopes, the spectra were calculated as the sum of the curves of species containing isotope ^{63}Cu or ^{65}Cu weighted by their natural abundances, where the higher hyperfine coupling of ^{65}Cu was taken into account. The hyperfine coupling constants and the relaxation parameters are given in gauss (G) units (1 G = 10^{-4} T) for the major isotope ^{63}Cu throughout the paper.

The quality of fit for the jth spectrum was characterized by the noise-corrected regression parameter R_j, computed from the average square deviation for the curve in question to obtain $R_j = 1$ for a perfect fit, when the quadratic error of the fit is equal to the noise obtained from the wings of the spectrum. For the overall set of spectra, the quality of fit was given by the overall regression parameter R, which is calculated from the sum of the average square deviation values. The details of the statistical analysis were reported previously.[14]

2.5. Analysis of ESR Spectra in Frozen Solution. The anisotropic ESR spectra were evaluated by using the EPR program,[25] which allows a description of the experimental spectra as a superposition of two component curves. The spectral fits (characterized by the noise-corrected regression parameter R_j, see above) achieved with the assumption of either axial or rhombic g, hyperfine, and quadrupole coupling tensors were compared with each other to gain information on the symmetry of the coordination polyhedra in various species. In some cases, the spectral fits achieved with different numbers of N nuclei in the coordination sphere were also compared. Anisotropy of the relaxation parameters and the strain dependence of α, β and γ were additionally taken into consideration. The calculated spectra were composed from the curves of the complexes containing the isotope ^{63}Cu or ^{65}Cu, as for the isotropic spectra.

3. Results and Discussion

3.1. Equilibrium Model in the Cu(II)−3-Pyridylmethanol System. The simple model including the metal complexes $[Cu(aqua)]^{2+}$, $[CuL]^{2+}$, $[CuL_2]^{2+}$, $[CuL_3]^{2+}$ and $[CuL_4]^{2+}$, identified by pH potentiometry,[26] proved to be satisfactory for a good description of the series of isotropic ESR spectra (Figure 1). The formation constants for the various species, together with the corresponding literature data, are given in Table 1. The agreement between the values obtained by ESR evaluation and by pH potentiometry is excellent. The distribution of Cu(II) among the various complexes, calculated from the set of formation constants under the conditions of the ESR titrations, is depicted in Figure 2, which indicates the moderate stability of various species, particularly $[CuL_3]^{2+}$ and $[CuL_4]^{2+}$: the latter is formed in less than 20% relative concentration, even at a 0.1 M ligand concentration.

3.2. ESR spectra in the Cu(II)−3-Pyridylmethanol System at 298 K. The ESR parameters determined by 2D analysis of the spectrum series are also listed in Table 1, and the corresponding spectra calculated from these data are presented in Figure 3. The most striking feature is the considerable line width accompanied by an unusual, "irregular" shape, particularly for $[CuL_3]^{2+}$. For $[Cu(aqua)]^{2+}$ and $[CuL]^{2+}$ with high g_0, the broad lines are not surprising, as the relaxation parameter α is proportional to the square of the g-anisotropy. However, for the mononuclear complexes of chelating ligands with g_0 similar to that of $[CuL_2]^{2+}$ in the present system, a well-resolved hyperfine splitting is typical.[14−21,27] Questions arise as to whether (1) the distortion of the spectra is caused by the incomplete averaging of the anisotropy of the magnetic parameters, or (2) the distortion is due to an exchange interaction between metal ions connected by 3-pyridylmethanol bridges, or (3) the slow exchange criterion is not fulfilled (i.e., the lifetime of the labile complexes is of the order of the relaxation time (10^{-8} s)). The first explanation is unlikely, as neither the size of the complex molecules nor the viscosity of the solution can appreciably inhibit the rotation of various species relative to other systems with "regular" spectra.[14−21,27] If the broad, irregular spectral shapes originated from the interactions of metal ions bridged by the ligand molecules, this feature of the curves would remain

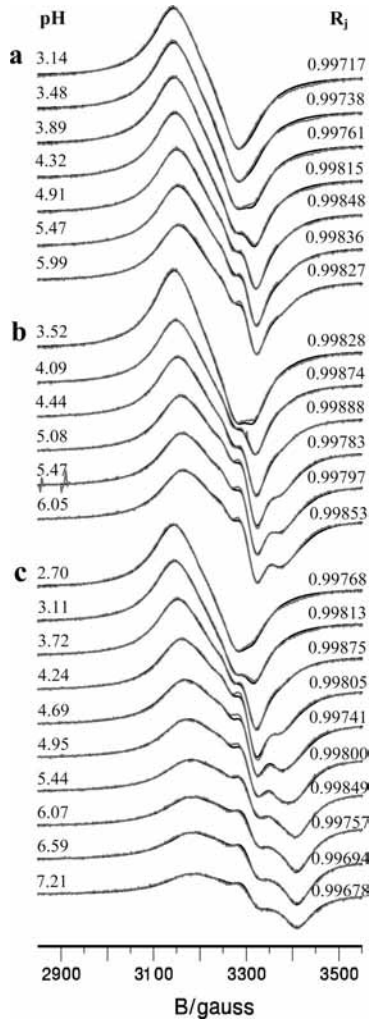

Figure 1. Experimental (gray line) and calculated (black line) spectra at 298 K: (a) $T_{Cu} = 5$ mM, $T_L = 10$ mM; (b) $T_{Cu} = 5$ mM, $T_L = 25$ mM; (c) $T_{Cu} = 5$ mM, $T_L = 100$ mM. The overall regression parameter R is 0.99821 for the series of spectra.

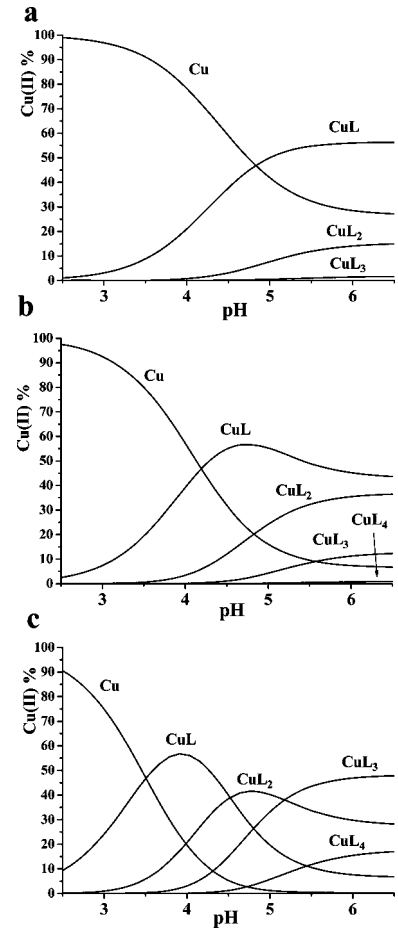

Figure 2. Concentration distribution of the Cu(II) ion among the various species (charges omitted) calculated from the formation constants in Table 1: (a) $T_{Cu} = 5$ mM, $T_L = 10$ mM; (b) $T_{Cu} = 5$ mM, $T_L = 25$ mM; (c) $T_{Cu} = 5$ mM, $T_L = 100$ mM.

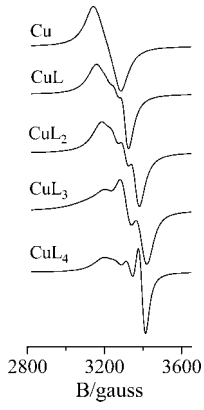

Figure 3. Spectra calculated at 9.87 GHz from the isotropic ESR parameters in Table 1 for the species (charges omitted) identified in the Cu(II)−3-pyridylmethanol system.

or even be enhanced at low temperature, as the decrease of temperature promotes the association of molecules, whereas the anisotropic spectra are well-resolved and characteristic of mononuclear complexes (see in detail in section 3.3), and thus the second possible explanation should also be rejected. Accordingly, the possible structures and the rates of their interconversions must be considered in an attempt to explain the distortion of the ESR spectra at 298 K.

3.3. Coordination Modes at 298 K. In parallel with an increase in the number of organic ligand molecules in the various complexes, a decrease in g_0 and an increase in A_0 are to be expected, as a consequence of the stronger equatorial ligand field caused by the increasing number of N donors. This trend can be observed only for $[Cu(aqua)]^{2+}$, $[CuL]^{2+}$ and $[CuL_2]^{2+}$: there is a break-point with $[CuL_3]^{2+}$ (Table 1). This suggests the presence of isomers which contain one N donor atom in an axial rather than an equatorial position. A similar phenomenon has been reported for a number of other systems.[14,15,17,18]

$[CuL_2]^{2+}$ may be a mixture of two coexisting geometric isomers that differ from each other in the *cis* or *trans* arrangement of the two equatorial N donors (Figure 4). For these species, similar ligand fields and g_0 values are likely, whereas the isomer with lower symmetry is expected to have a smaller A_0 as a consequence of the slight rhombic distortion: such a *cis*−*trans* isomerism has been demonstrated for chelate complexes[19,27] and probably occurs for this 3-pyridylmethanol complex too. It is worth mentioning that *cis*−*trans* isomerism has not been identified in solid Cu(II) complexes involving only monodentate ligands. For $[CuL_3]^{2+}$ and $[CuL_4]^{2+}$, besides the 3N and 4N isomers with lower g_0, respectively, 2N and 3N isomers with higher g_0, with one N in an axial position, are also likely to form (Figure 4). Moreover, for $[CuL_3]^{2+}$, the equatorial N donors of the 2N isomer can be bound in either *cis* or *trans* positions, finally resulting in three possible coordination modes (Figure 4). The poorly resolved spectra, however, do not allow further deconvolution in the system

TABLE 1: Isotropic ESR Parameters[a] and Formation Constants as log β for the Cu(II) Complexes of 3-Pyridylmethanol at 298 K

complex	g_0	A_0/G	a_{No}/G	α/G	β/G	γ/G	log β	log β^b
LH							5.08[b]	5.08
$[Cu(aqua)]^{2+}$	2.1947(1)	34.4(1)		54.5(2)	−2.0(1)	0.69(8)		
$[CuL]^{2+}$	2.1751(1)	41.7(1)	1.0(12)	51.2(1)	−7.2(1)	−0.60(5)	2.60(1)	2.45
$[CuL_2]^{2+}$	2.1477(2)	49.6(2)	6.0(8)	47.2(3)	−7.3(2)	2.43(11)	4.30(1)	4.30
$[CuL_3]^{2+}$	2.1488(4)	70.3(6)	14.7(14)	48.0(7)	−32.4(1)	16.19(7)	5.61(1)	5.63
$[CuL_4]^{2+}$	2.1313(6)	55.7(8)	6.4(9)	47.7(4)	−15.8(5)	0.38(3)	6.24(2)	6.35

[a] The confidence intervals of the parameters as regards the last digit(s) are given in parentheses. The hyperfine coupling constants and the relaxation parameters are given in G (10^{-4} T) units and refer to the isotope ^{63}Cu. [b] Reference 26.

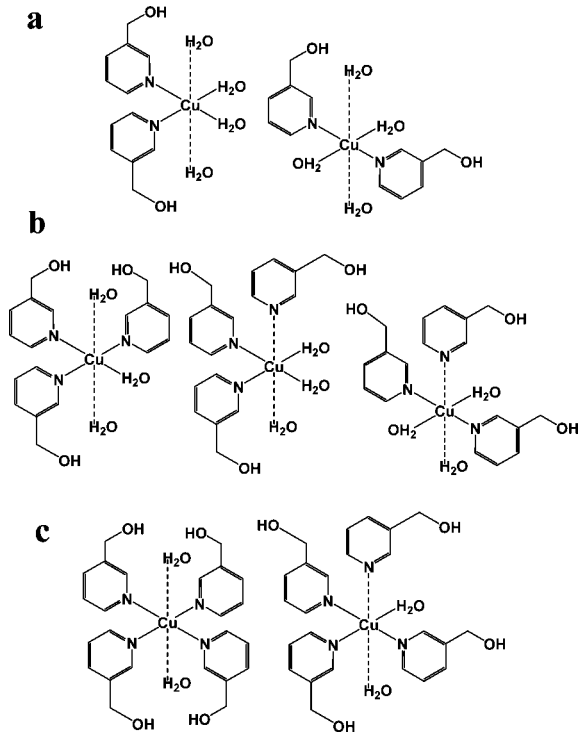

Figure 4. Possible coordination modes: (a) $[CuL_2]^{2+}$; (b) $[CuL_3]^{2+}$; (c) $[CuL_4]^{2+}$.

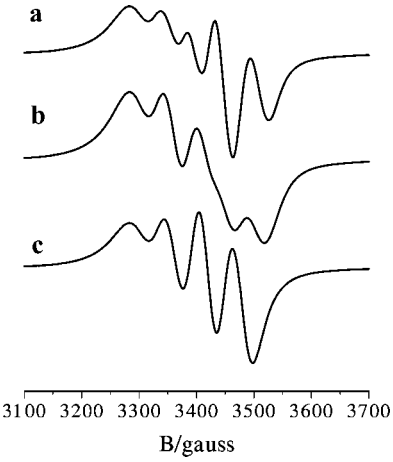

Figure 5. ESR spectra calculated for the interconversion of two complexes. For the first one, $g_0 = 2.150$, $A_0 = 48$ G, $a_{No}(2N) = 10$ G, and the mole fraction is 0.5; for the second one, $g_0 = 2.130$, $A_0 = 64$ G, $a_{No}(3N) = 10$ G, and the mole fraction is 0.5; for both, $\alpha = 25$ G, $\beta = -8$ G, $\gamma = 4$ G; their lifetimes are (a) 1000 ns, (b) 5 ns, and (c) 1 ns.

studied: attempts to take more species into consideration were unsuccessful, resulting in nonunique resolution and uncertain parameters.

The interconversions of the above species require ligand exchange, which is faster for monodentate ligands than for chelate complexes. This is one of the reasons for the distortion of the spectra through the partial breakdown of the slow-exchange criterion. The effect of the lifetime of the exchanging species on the spectral shape is illustrated in Figure 5, where the two component spectra are calculated from the averages of the principal values of g and the hyperfine coupling tensors for $[CuL_2]^{2+}$ and $[CuL_3]^{2+}$ obtained by the simulation of the spectra at 77 K (see below), using line width parameter values typical for well-resolved isotropic spectra of Cu(II) complexes in fluid media. Comparison of these curves reveals how the linear superposition of the component spectra (top) is broadened and distorted (middle) until the coalescence of the two spectra occurs (bottom) as the lifetime decreases. There are two species that can simply interconvert through the elongation or shortening of certain bonds: the 3N and the *trans*-2N isomers of $[CuL_3]^{2+}$ (Figure 4). The latter process is certainly faster than the ligand exchange, causing a more significant deviation from the criterion of slow exchange, which will yield an incorrect spectrum shape in the decomposition procedure for the species in question (Figure 3). For comparison, in the case of *tris* complexes of small bidentate chelating ligands forming five-membered rings with Cu(II), the typical time of the Jahn−Teller inversion is approximately 10 ns, as obtained from NMR relaxation studies.[22]

3.4. Anisotropic ESR Spectra for the Cu(II) Complexes of 3-Pyridylmethanol. The majority of the spectra taken in frozen solution at 77 K exhibit a superimposed character (Figure 6), in accordance with the distribution curves (Figure 2), which reflect the simultaneous formation of several complexes under various conditions. Surprisingly, at a 20-fold excess of ligand and pH > 4.7, the spectra do not change with variation of the pH, and seem one-component curves. This suggests that one strongly predominant species is likely to be present, though at 298 K these solutions contain all the complexes in varying concentrations (except for $[Cu(aqua)]^{2+}$). Fortunately, the well-resolved N superhyperfine splitting furnishes an excellent opportunity for computer simulation to obtain the number of N donors occupying equatorial sites (as the spectra indicate the $d_{x^2-y^2}$ ground state), and to identify the species in question.

Simulations with the assumption of 2, 3 or 4 N donors and axial or rhombic g and hyperfine coupling tensors were carried out for these one-component spectra. The 2N model gave an unsatisfactory spectral fit for both symmetries. For the 3N and 4N models, the R_j values were nearly equal for the axial and rhombic symmetries, when the rhombic model resulted in approximately coinciding principal values of the g and hyperfine coupling tensors (when different g_{xx} and g_{yy}, A_{xx} and A_{yy}, etc. values were given, the fit deteriorated significantly, and the differences were again reduced during the subsequent optimization procedure, giving better and better R_j values). This means

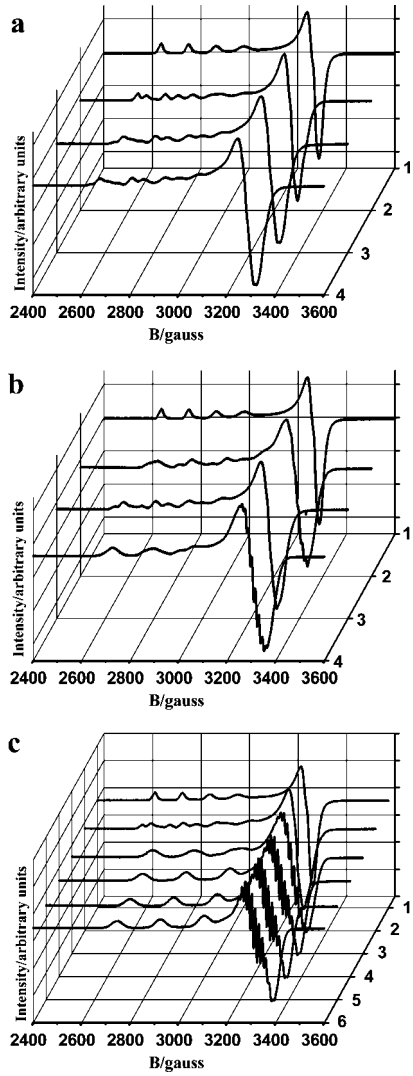

Figure 6. Experimental spectra at 77 K: (a) $T_{Cu} = 5$ mM, $T_L = 10$ mM, pH = 2.31, 3.89, 4.91 and 5.99 from 1 to 4, respectively; (b) $T_{Cu} = 5$ mM, $T_L = 25$ mM, pH = 2.08, 4.09, 5.08 and 6.05 from 1 to 4, respectively; (c) $T_{Cu} = 5$ mM, $T_L = 100$ mM, pH = 1.83, 3.11, 4.24, 4.63, 4.95 and 6.07 from 1 to 6, respectively.

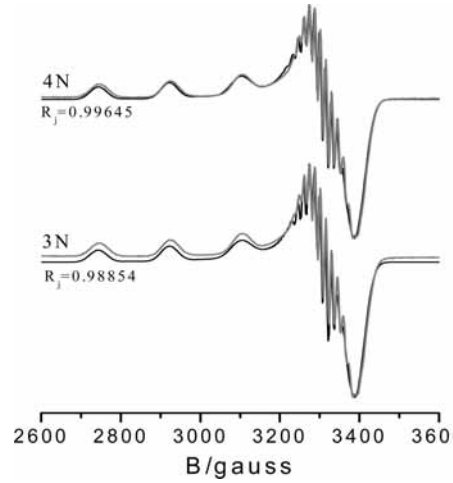

Figure 7. Experimental spectrum at 77 K, $T_{Cu} = 5$ mM, $T_L = 100$ mM, pH = 7.21 (gray line), together with the spectra calculated with axial symmetry assuming 4N (top) or 3N (bottom) superhyperfine splitting (black lines).

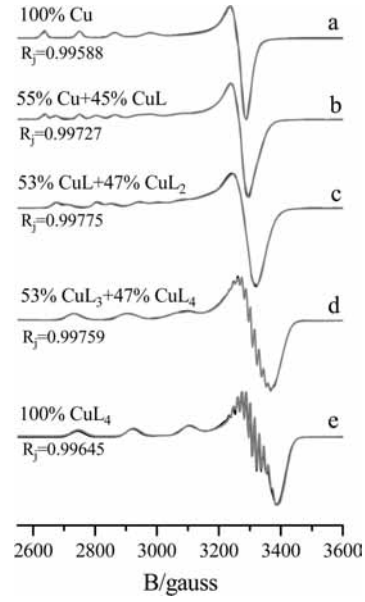

Figure 8. Experimental (gray line) and calculated (black line) spectra at 77 K: (a) $CuCl_2$ solution; (b) $T_{Cu} = 5$ mM, $T_L = 10$ mM, pH = 3.89; (c) $T_{Cu} = 5$ mM, $T_L = 10$ mM, pH = 4.91 after the subtraction of the Cu(II) spectrum with a weighting factor of 0.16; thus, in the frozen solution the distribution was 16% Cu, 44% CuL, 40% CuL_2; (d) $T_{Cu} = 5$ mM, $T_L = 100$ mM, pH = 4.24; (e) $T_{Cu} = 5$ mM, $T_L = 100$ mM, pH = 4.69. In all cases, axial symmetry was assumed. The charges of the complexes are omitted.

the occurrence of axial symmetry for the complex in question. The experimental curve shown in Figure 7, together with the spectra calculated according to the axial model, illustrates the difference between the 3N and 4N superhyperfine patterns. For the latter, the fit is quite good, indicating that the solution at 77 K contains a predominant complex with a symmetric structure, with 4 N donors in equatorial positions. This species should be the complex $[CuL_4]^{2+}$, though in the corresponding solutions at 298 K it is present in a relative concentration of merely 2−16%.

Some other anisotropic spectra were also simulated (Figure 8), taking into consideration one or two component spectra. (In the case of spectrum 3 in Figure 6a, the third component was clearly $[Cu(aqua)]^{2+}$; the experimental spectrum of the latter was simply subtracted from the above-mentioned experimental curve in a ratio that ensured the disappearance of its low-field lines for the visual comparison. The modified curve could then be described well as a two-component one; Figure 8c. The parameters of the component assigned to $[CuL]^{2+}$ were in good agreement with those determined from the experimental curve in Figure 8b.) For all the above selected spectra, a good spectral fit could be achieved with one or two component curves relating to axial symmetry. The presence of other, minor species cannot be excluded, though their concentrations certainly remain below 10% (the omission of species in concentration of over 10% would cause a significant deterioration of the fit). The ESR parameters for the various species are reported in Table 2, and the corresponding calculated spectra are depicted in Figure 9.

Comparison of the concentration ratios at low temperature (Figure 8) with those in fluid solution (Figure 2) reveals that the formation of species containing larger numbers of organic ligands becomes more favored at low temperature; besides, the isomeric equilibria are shifted toward the molecules containing all N donor atoms in equatorial positions, as suggested by the anisotropic g principal values and their averages, which are lower than in fluid solution and display a decrease with increasing number of organic ligand molecules in the complex

TABLE 2: Anisotropic ESR Parameters[a] for the Predominant Cu(II) Complexes of 3-Pyridylmethanol at 77 K

complex	$g_\perp$	$g_\parallel$	g_0[b]	$A_\perp$/G	$A_\parallel$/G	A_0[b]/G	$a_{N\perp}$/G	$a_{N\parallel}$/G	$P_\parallel$/G
$[Cu(aqua)]^{2+}$	2.0794(1)	2.4216(5)	2.1935(5)	1.86(2)	111.6(1)	38.4(1)			4.1(1)
$[CuL]^{2+}$	2.0683(4)	2.3677(8)	2.1680(9)	0.59(1)	129.3(1)	43.5(1)	7.6(2)	5.9(2)	8.6(4)
$[CuL2]^{2+}$	2.0632(1)	2.3288(2)	2.1517(2)	2.27(2)	138.2(2)	47.6(2)	12 (fixed)	7 (fixed)	9.1(5)
$[CuL3]^{2+}$	2.0594(1)	2.2874(3)	2.1354(3)	14.00(1)	162.7(2)	63.6(2)	13.8(1)	8.8(3)	5.8(11)
$[CuL4]^{2+}$	2.0497(1)	2.2575(3)	2.1190(3)	17.51(4)	175.0(2)	70.0(3)	14.3(1)	9.7(2)	8.3(1)

[a] The confidence intervals of the parameters as regards the last digit(s) are given in parentheses. The hyperfine coupling constants and the relaxation parameters are given in G (10^{-4} T) units and refer to the isotope ^{63}Cu. [b] Average of the principal values given in this.

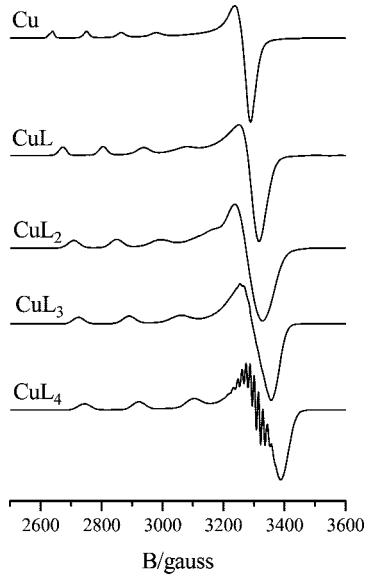

Figure 9. Spectra calculated at 9.52 GHz from the anisotropic ESR parameters in Table 2 for the species (charges omitted) identified in the Cu(II)−3-pyridylmethanol system.

(Table 2). This trend is expected in terms of the van't Hoff equation $\ln K_2 = \ln K_1 - \Delta H/R(1/T_2 - 1/T_1)$, because the formation enthalpy ΔH becomes more and more negative as the weak Cu−O(aqua) bonds are progressively replaced by the stronger Cu−N bonds in the equatorial plane, making the formation of $[CuL_3]^{2+}$ and particularly $[CuL_4]^{2+}$ favored at low temperature. The measure of the change in distribution, however, is unusual: only a few examples[27,28] are known, which indicate considerable alterations upon freezing. It is worth mentioning that for amino acid and peptide complexes, in most cases, the concentration distribution in the glassy samples corresponds to a pH lower by 0.3−0.5 than in the fluid state,[28,29] i.e., for those equilibrium systems the differences in the formation enthalpies are masked by the decrease of pH upon freezing.

According to the solid−liquid phase diagram for the methanol−water system, obtained by differential scanning calorimetry,[30] the freezing of a 25 v/v % methanol−water mixture begins at about 257 K under equilibrium conditions. The question arises as to whether the concentration distribution in the copper(II)−3-pyridylmethanol system corresponds to this temperature or undercooling of the solution occurs in the course of fast freezing. The formation enthalpy values are not known for the above system; however, they were determined for the Cu(II) complexes of pyridine.[31] The coordination of 3-pyridylmethanol is pyridine-like (see above), even the formation constants of $[CuL]^{2+}$, $[CuL_2]^{2+}$, $[CuL_3]^{2+}$, and $[CuL_4]^{2+}$ with pyridine,[31−35] 2.54(3), 4.39(7), 5.62(28), and 6.43(22), respectively, agree with those of the corresponding 3-pyridylmethanol complexes within experimental error (Table 1). Therefore, the formation enthalpy values for the pyridine complexes[31] (−16.8, −37.2, −67.3, and −92 kJ/mol in the above order) seem to be good estimates for the 3-pyridylmethanol complexes too and can be used reasonably for the calculation of their temperature dependent formation constants.

The distribution of Cu(II) among $[Cu(aqua)]^{2+}$, $[CuL]^{2+}$, $[CuL_2]^{2+}$, $[CuL_3]^{2+}$ and $[CuL_4]^{2+}$, calculated from the sets of formation constants obtained from the van't Hoff equation at various temperatures, is in satisfactory agreement with the concentrations determined by the analysis of the anisotropic spectra if 230 K < T_2 < 240 K is assumed. For the solutions yielding the spectra in Figure 8b−e in frozen state, the mol % concentrations of the above five species obtained at 233 K are [46, 41, 11, 2, 0], [16, 39, 29, 14, 2], [0, 2, 9, 45, 44], and [0, 0, 3, 33, 64], respectively. Both at higher and at lower temperature, the agreement is much worse. In other words, the complex equilibria of Cu(II) and 3-pyridylmethanol "are frozen" in the temperature interval 230−240 K. Though the experimental errors, neglected minor species, the decrease of pH upon freezing, and other approximations afford only a rough estimation, the results support significant undercooling of the solution in the course of fast freezing applied to obtain well-resolved anisotropic spectra in the glassy samples.

4. Conclusions

For the Cu(II)−3-pyridylmethanol system in aqueous solution, the not too stable complexes $[CuL]^{2+}$, $[CuL_2]^{2+}$, $[CuL_3]^{2+}$, and $[CuL_4]^{2+}$ are formed up to pH = 7. The binding site of the ligand is the pyridyl N; coordination of the side chain and a bridging role of 3-pyridylmethanol cannot be detected. The *g* values indicate isomeric equilibria in which one of the isomers contains one ligand in an axial rather than an equatorial position, and *cis*−*trans* isomerism of the two equatorial N donors is also probable in $[CuL_2]^{2+}$, and $[CuL_3]^{2+}$ with the third N in an axial position. Relative to the complexes of chelating ligands, the isotropic spectra for this system reveal some line-broadening and distortion from the "regular" shape, which can be explained by a partial breakdown of the slow-exchange criterion. Freezing of the solution has an extremely high influence on the concentration distribution of the 3-pyridylmethanol complexes: the formation of $[CuL_3]^{2+}$, and particularly $[CuL_4]^{2+}$, is favored at low temperature at the expense of complexes containing fewer bound organic ligand molecules, and the isomeric equilibria are shifted toward the molecules in which all the N donors occupy equatorial positions. This can be attributed to the larger number of Cu−N bonds leading to a favorable enthalpy term on the one hand, and the dramatic decrease of the congelation temperature of the solution on the other hand, in particular when a solvent of low freezing point is mixed with water to promote glass formation. We emphasize the importance of the latter effect, which is often underestimated in the literature when fast freezing is applied.

Acknowledgment. This work was performed in the framework of a Hungarian-Slovak Intergovernmental S&T Coopera-

tion (Grant TéT SK-25/2006). The financial support of the Hungarian Scientific Research Fund OTKA (Grant K-72781) and the Slovak Fund VEGA 1/0353/08 is likewise gratefully acknowledged.

References and Notes

(1) Weder, J. B.; Dillon, C. T.; Hambley, T. W.; Kennedy, B. J.; Lay, P. A.; Biffin, J.; Regrop, H. L.; Davies, N. M. *Coord. Chem. Rev.* **2002**, *232*, 95.

(2) Melník, M.; Smolander, K.; Sharrock, P. *Inorg. Chim. Acta* **1985**, *103*, 187.

(3) Klenka, L.; Klima, M. *Cesk. Oftalmol.* **1952**, *8*, 123.

(4) Kopelevich, V. M.; Gunnar, V. I. *Pharm. Chem. J.* **1999**, *33*, 177.

(5) Hendrix, C. Patent WO/2007/053773.

(6) Gryglewski, R. J.; Botting, R. M.; Vane, J. R. *Hypertension* **1988**, *12*, 530.

(7) Svik, K.; Stančíková, M.; Rovenský, J.; Melník, M. *Rheumatologia* **1995**, *9*, 89.

(8) Stachová, P.; Korabik, M.; Koman, M.; Melník, M.; Mrozinski, J.; Glowiak, T.; Mazúr, M.; Valigura, D. *Inorg. Chim. Acta* **2006**, *359*, 1275.

(9) Marošová, J.; Moncol', J.; Koman, M.; Melník, M.; Glowiak, T. *Acta Crystallogr.* **2006**, *E62*, m3385.

(10) Moncol', J.; Segl'a, P.; Mikloš, D.; Mazúr, M.; Melník, M.; Glowiak, T.; Valko, M.; Koman, M. *Polyhedron* **2006**, *25*, 1561.

(11) Jašková, J.; Mikloš, D.; Segl'a, P.; Sillanpää, R.; Moncol', J. *Acta Crystallogr.* **2007**, *E63*, m9102.

(12) Moncol', J.; Maroszová, J.; Melník, M.; Koman, M. *Acta Crystallogr.* **2007**, *E63*, m114.

(13) Moncol', J.; Segl'a, P.; Jašková, J.; Fischer, A.; Melník, M. *Acta Crystallogr.* **2007**, *E63*, m698.

(14) Rockenbauer, A.; Szabó-Plánka, T.; Árkosi, Zs.; Korecz, L. *J. Am. Chem. Soc.* **2001**, *123*, 7646.

(15) Szabó-Plánka, T.; Nagy, N.; Rockenbauer, A.; Korecz, L. *Polyhedron* **2000**, *19*, 2049.

(16) Szabó-Plánka, T.; Árkosi, Zs.; Rockenbauer, A.; Korecz, L. *Polyhedron* **2001**, *20*, 995.

(17) Szabó-Plánka, T.; Nagy, N. V.; Rockenbauer, A.; Korecz, L. *Inorg. Chem.* **2002**, *41*, 3483.

(18) Nagy, N. V.; Szabó-Plánka, T.; Rockenbauer, A.; Peintler, G.; Nagypál, I.; Korecz, L. *J. Am. Chem. Soc.* **2003**, *125*, 5227.

(19) Árkosi, Zs.; Szabó-Plánka, T.; Rockenbauer, A.; Nagy, N. V.; Lázár, L.; Fülöp, F. *Inorg. Chem.* **2003**, *42*, 4842.

(20) Nagy, N. V.; Szabó-Plánka, T.; Tircsó, Gy.; Kiŕ; aly, R.; Árkosi, Zs.; Rockenbauer, A.; Brücher, E. *J. Inorg. Biochem.* **2004**, *98*, 1655.

(21) Fainerman-Melnikova, M.; Szabó-Plánka, T.; Rockenbauer, A.; Codd, R. *Inorg. Chem.* **2005**, *44*, 2531.

(22) Debreczeni, F.; Polgár, J.; Nagypál, I. *Inorg. Chim. Acta* **1983**, *71*, 195.

(23) Debreczeni, F.; Nagypál, I. *Inorg. Chim. Acta* **1983**, *72*, 61.

(24) Nagypál, I.; Debreczeni, F. *Inorg. Chim. Acta* **1984**, *81*, 69.

(25) Rockenbauer, A.; Korecz, L. *Appl. Magn. Reson.* **1996**, *10*, 29.

(26) Lenarcik, B.; Rzepka, M. *Pol. J. Chem.* **1981**, *55*, 503.

(27) Szabó-Plánka, T.; Gyurcsik, B.; Nagy, N. V.; Rockenbauer, A.; Šípoš, R.; Šima, J.; Melník, M. *J. Inorg/ Biochem/* **2008**, *102*, 101.

(28) Szabó-Plánka, T.; Peintler, G.; Rockenbauer, A.; Gyõr, M.; Varga-Fábián, M.; Institórisz, L.; Balázspiri, L. *J. Chem. Soc., Dalton Trans.* **1989**, 1925.

(29) Szabó-Plánka, T.; Rockenbauer, A.; Gyõr, M.; Gaizer, F. *J. Coord. Chem.* **1988**, *17*, 69.

(30) Takaizumi, K.; Wakabayashi, T. *J. Solution Chem.* **1997**, *26*, 927.

(31) Izatt, R.; Eatough, D.; Snow, R.; Christensen, J. *J. Phys. Chem.* **1968**, *72*, 1208.

(32) Bruehlman, R.; Verhoek, F. *J. Am. Chem. Soc.* **1948**, *70*, 1401.

(33) Leussing, D.; Hansen, R. *J. Am. Chem. Soc.* **1957**, *79*, 4270.

(34) Neves, E.; Peters, M. *Polyhedron* **1990**, *9*, 1257.

(35) Faraglia, G.; Rossotti, F.; Rossotti, H. *Inorg. Chim. Acta* **1970**, *4*, 488.

JP805210V